The Thermal Oxidation of Guayule and Hevea Rubbers by Dynamic Differential Scanning Calorimetry

M. A. PONCE-VÉLEZ and E. CAMPOS-LÓPEZ, *Centro de Investigación en Química Aplicada, Saltillo, Coahuila, Mexico*

Synopsis

The thermal oxidation of natural rubbers from *Hevea brasiliensis* (pale crepe and smoked sheet) and *Parthenium argentatum* (Guayule) were studied with differential scanning calorimetry (DSC) using the dynamic method. The atmosphere was oxygen at 110 ml/min and the temperature range was 393°–473°K. The decomposition reactions showed a pronounced exothermic emission with shoulders on the high-temperature side. The kinetic parameters were computed by using three different mathematical approaches: the heat evolution treatment of Borchardt and Daniels, the diffusion-controlled method by Jander, and the heating rate method developed by Kissinger and Ozawa. The best agreement between these methods was achieved assuming first order in the Borchardt and Daniels method and three-dimensional diffusion with the Jander model. The mass influence was analyzed observing that good agreement is obtained working with sample weight in the order of 3–4 mg. Under such conditions the activation energies (E_a) were 16–17, 18–19, and 23–24 kcal/mole for the Borchardt-Daniels, Kissinger-Ozawa, and Jander models, respectively.

INTRODUCTION

The thermal degradation of polymeric materials is a topic extensively studied in recent years[1–5] using thermal techniques such as differential scanning calorimetry (DSC), differential thermal analysis (DTA), and thermogravimetry (TGA). Usually the experiments are carried out in inert atmospheres in order to avoid interference with oxidation reactions, since thermal scissions are relatively easy to follow.

With natural or synthetic elastomers, the thermal oxidation behavior is more relevant from the point of view of its stability and the relationship obtained with the performance of the material. Several methods are used to investigate the oxidation behavior of rubbers under accelerated conditions, such as infrared spectroscopy,[6,7] oxygen absorption,[8] or the decay in some mechanical property.[9,10] With the development of more sophisticated calorimetric techniques a new field of applications was developed which is related to the oxidation of elastomers and to the evaluation of antioxidants,[11] among others. However, the oxidation reactions in unsaturated polymers are difficult to interpret[12] mainly because of the presence of parallel reactions and a complex mechanism.

There are several papers on the kinetics of thermal oxidation of natural Hevea rubber (NR) using infrared spectroscopy,[6] reporting values of 20 kcal/mole for the activation energy E_a involved in such processes. In the case of Guayule rubber (GR), there are no reported values on this specific subject, principally due to its lack of commercial interest. However, both rubbers show identical microstructure,[13,14] mainly *cis*-1,4, and they should present similar thermo-oxidation patterns.

Journal of Applied Polymer Science, Vol. 22, 2485–2497 (1978)

0021-8995/78/0022-2485$01.00

There are two alternatives in the study of the kinetics of thermal oxidation by thermal analytic techniques: the isothermal method, in which the sample is maintained at a constant temperature throughout the experiment, and the dynamic mode, where the material is degraded at a programmed heating rate. The dynamic mode presents several advantages mainly due to shorter running times.

A typical exotherm is presented in Figure 1, where the total area A is directly proportional to the total heat ΔH generated during the oxidation process of total mass m_0 and a represents the partial area related to the heat evolved during time t by the mass m. The analysis of these variables as a function of time might be used to calculate the kinetic features, however, the mathematical model is one of the most important aspects, and later on, some of the developments will be discussed.

Using the dynamic mode to measure the kinetics of depolymerization, there are several reports on the manipulation of experimental data to calculate parameters such as activation energy E_a, the apparent reaction order x, and the rate of reaction constant k. A brief description of the most important models is presented below.

Heat Evolution. This is one of the most common methods and consists in measuring the reaction heat as a function of temperature related to the time t. This method was first developed by Borchardt and Daniels[15] for solutions, and after that Uricheck[19] used the same principle on solids. The method is based on the determination of the heat of reaction from the exotherm as a function of temperature, and it applies to first-order reactions of nonvolatile materials. However, some systems are of such complexity that this reduced scheme is oversimplified and gives erroneous results[20] for E_a.

The general equation derived for this treatment is

$$k_x = \frac{(A/m_0)^{x-1} dH/dt}{(A - a)^x} \tag{1}$$

where k_x is the rate constant of a reaction of order x, dH/dt is the heat evolved at time interval dt, A is the total area under the exotherm and is proportional to the total heat evolved during the reaction, and a is the area covered during

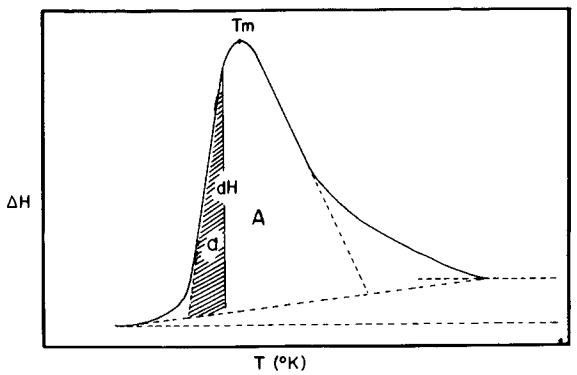

Fig. 1. Typical DSC thermogram of the thermal oxidation of natural rubbers and the variables used for the calculation of kinetic values.

the time t corresponding to the heat of reaction of a mass m. By using the Arrhenius equation, the activation energy might be calculated from

$$\frac{\Delta \ln k}{\Delta(1/T)} = \frac{E_a}{R} \tag{2}$$

Equation (1) is strongly dependent on the reaction order which is a factor of inaccuracy principally in multistep reactions; and according to Mackenzie[21] there is no significance except in the mathematical formulation.

These statements are based on reactions involving the liquid state, where the reaction order might have any value. However, with solid samples only reactions with $x = 0$, $\frac{1}{2}$, $\frac{2}{3}$, and 1.0 have theoretical justification. The conversion rate is a function of

$$\frac{d\alpha}{dt} = k f(\alpha) \tag{3}$$

where $\alpha = (m_0 - m)/m_0$. Borchardt used the equation

$$\frac{d\alpha}{dt} = k(1 - a)^x \tag{4}$$

with values of $x = 0$, $\frac{1}{2}$, $\frac{2}{3}$, and 1.0, and introduced enthalpy variations with respect to time and derived the following expressions:

$$k_0 = \frac{dH/dt}{A} \qquad x = 0 \tag{5}$$

$$k_{1/2} = \frac{dH/dt}{2A[1 - (a/A)]^{1/2}} \qquad x = \tfrac{1}{2} \tag{6}$$

$$k_{2/3} = \frac{dH/dt}{3A[1 - (a/A)]^{2/3}} \qquad x = \tfrac{2}{3} \tag{7}$$

$$k_1 = \frac{dH/dt}{A - a} \qquad x = 1.0 \tag{8}$$

These are equations that are used in the calorimetric determinations of kinetics of solid-state reactions.

Controlling Diffusion. By using the general eq. (3), a function can be established in terms of diffusion arguments. A review by Skvara and Satava[22] shows mathematical approaches for different types of diffusion process:

$$\alpha^2 = kt \tag{9}$$

$$(1 - \alpha) \ln (1 - \alpha) + \alpha = kt \tag{10}$$

$$[1 - (1 - \alpha)^{1/3}]^2 = kt \tag{11}$$

$$(1 - \tfrac{2}{3}\alpha) - (1 - \alpha)^{2/3} = kt \tag{12}$$

Equation (9) corresponds to a one-dimensional diffusion process, eq. (10) represents a two-dimensional process, eq. (11) was derived by Jander[23] and represents a three-dimensional process with spherical symmetry, and finally eq. (12) is also representative of a three-dimensional diffusion process. These equations can be transformed to expressions involving calorimetric terms; using eq. (11) this can be converted to the following expression:

$$k_3 = \frac{2(dH/dt)}{3A} \frac{1 - [1 - (a/A)]^{1/3}}{[1 - (a/A)]^{2/3}} \tag{13}$$

This equation will be used for the computation of the experimental data shown in the results.

Heating Rate Method. The peak in an exotherm occurs when the reaction rate is at a maximum, and it is possible to calculate kinetic variables directly from calorimetric data by running a number of decomposition patterns at different heating rates β. Kissinger[17] working with inorganic materials performed measurements on kinetic behavior and derived the mathematical framework necessary to calculate the activation energy by varying β and measuring the displacement of the peak T_m. Ozawa[18] discussed some methods used in order to avoid unrealistic results and agreed that one possible way to avoid errors is to carry out the experiments at several heating rates. A general equation was deduced for such methods:

$$\frac{\Delta \log \beta}{\beta(1/T_m)} = 0.457E_a/R \tag{14}$$

where β is given in °K/min, 0.457 is a factor obtained from the mathematical deduction, R is the universal gas constant in kcal, and E_a is the activation energy. By plotting log β against $1/T_m$, a straight line is obtained whose slope is proportional to E_a.

EXPERIMENTAL

Materials

***Hevea brasiliensis* Rubber.** Pale crepe and smoked sheet were used in the experiments. To eliminate traces of antioxidants and impurities, the rubber was cut in thin pieces and dissolved in benzene. The solution was filtered, the rubber was coagulated in acetone and redissolved, and the procedure repeated four times. The small rubber crumbs were dried under vacuum at 40°C for 72 hr. Dried rubber was dissolved in THF to obtain a 1% (weight/volume) solution from which films were cast under nitrogen atmosphere and dried under vacuum.

***Parthenium argentatum* Rubber.** Guayule shrub recently harvested was defoliated and milled in a hammer mill, defibrated in a blender for 5 min, and floated in water. Rubber "worms" obtained were skimmed out and deresinated in acetone several times. In order to ensure complete deresination and to eliminate foreign insoluble matter, the "worms" were dissolved in benzene, filtered through a Millipore filter three times, and coagulated with acetone. The coagulated rubber was dried under vacuum at 40°C for 72 hr and a 1% he-THF solution was prepared; films were cast on glass under nitrogen atmosphere and dried under vacuum at room temperature.

Calorimetric Determinations

Specimens. The films obtained were folded and pressed between stainless steel plates in a Carver press under a pressure of 5 tons. Specimens weighing 14–15 mg were cut into regular small disks and placed into the aluminum pans. Samples weighing 3–4 mg were not pressed.

Differential Scanning Calorimetry. A du Pont thermal analyzer Model

990 equipped with a differential scanning calorimeter module was used in these experiments. The du Pont DSC uses a constantan plate with two small platforms, one for the sample and one for a reference, in this case an empty aluminum pan. For calibration of the instrument, several standards were used (zinc, tin, and lead) measuring the area generated during the melting of a mass and using the following equation for the determination of ΔH:

$$\Delta H = 60\, ABE\, \Delta q_s/m$$

where ΔH is the enthalpy in mcal/mg, A is the area in square inches, B is the speed of the recorder, E is the calibration constant, Δq_s is the sensitivity in mcal/sec-in., and m is the sample mass in mg.

The oxygen atmosphere was maintained at a constant flow of 110 ml/min using a Nupro valve and was periodically measured by the soap bubble method commonly used in gas chromatography.

RESULTS AND DISCUSSION

Degradation reactions in natural rubbers studied by dynamic Differential Scanning Calorimetry (DSC) show well defined exothermic emissions which can be used to analyze the kinetics of the decomposition, however, the experimental conditions are very important factors in affecting the accuracy of the experiments, among the most important are the heating rate, atmosphere and sample—mass.

The effect of the atmosphere on rubber degradation is shown in Figure 2, where the remarkable change in degradation pattern can be noticed using two different types of environment: one inert with nitrogen and the other with dynamic oxidative atmosphere. Mass influence is also an important factor to be considered mainly if a quantitative study is pursued. Figure 3 presents thermograms obtained with two different masses: 14.0–15.0 and 3.0–4.0 mg. Remarkable differences are noticed reflected in variations in ΔH values. When a smaller mass is used, the enthalpy of the thermal oxidation for the three rubbers are in close

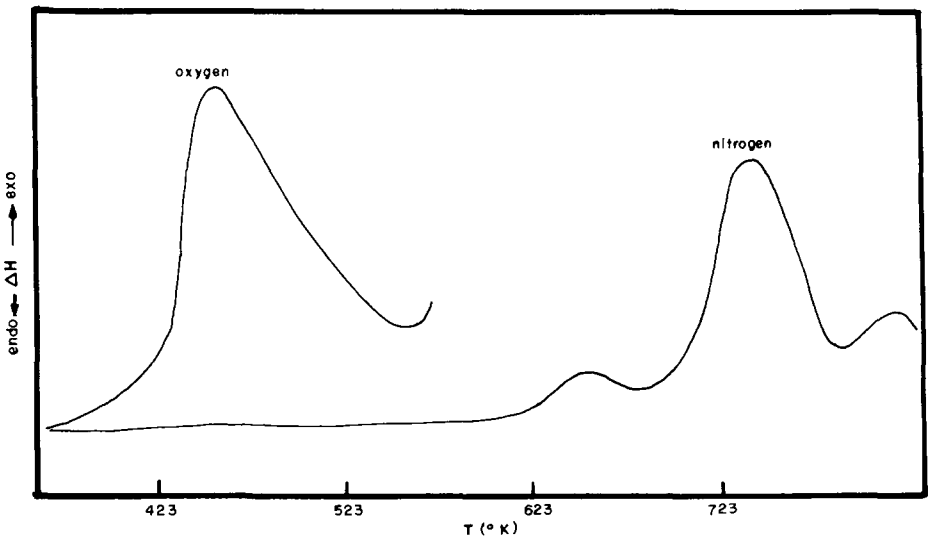

Fig. 2. Atmosphere effect on the degradation of natural rubber.

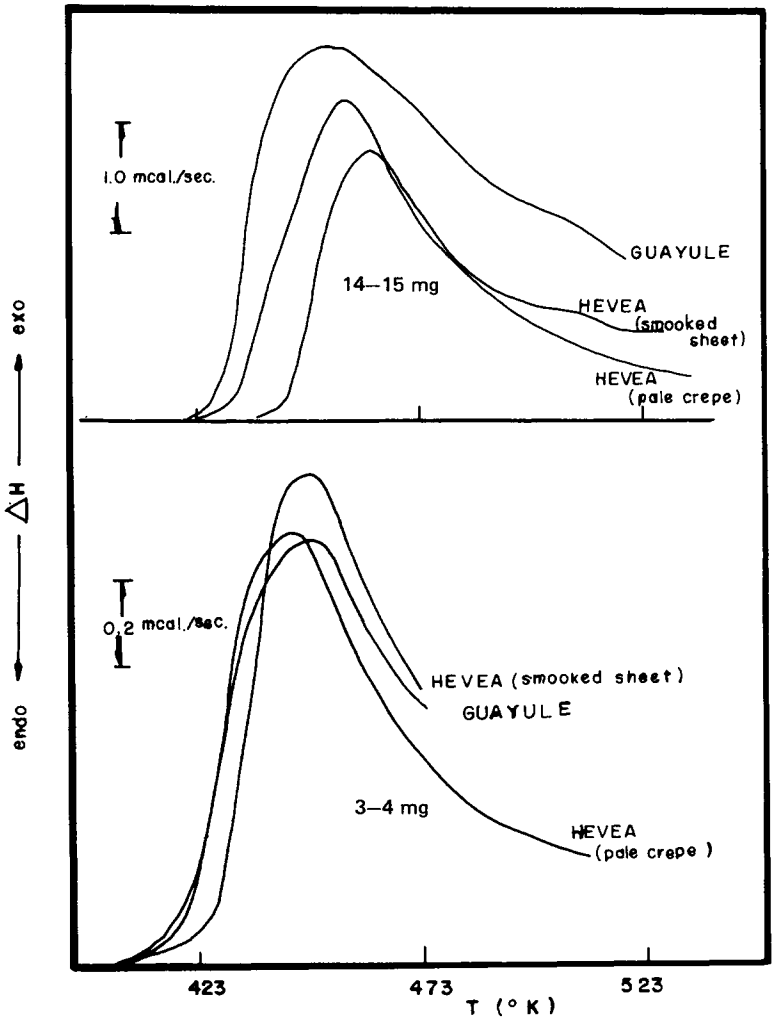

Fig. 3. Thermograms of natural rubbers showing the influence of sample mass. Atmosphere was oxygen at a flow rate of 110 ml/min, and heating rate was 5°C/min.

agreement, as can be observed in Table I. The effect of mass should be considered when the exotherm profile is going to be used to calculate the kinetics of the reaction.

Varying the heating rate β, a peculiar displacement is observed in the peak temperature; simultaneously, a broadening on the termogram is noticed on the high-temperature side, this effect being stronger in Guayule rubber. In Figure

TABLE I
Influence of Sample Mass on the Thermal Oxidation Enthalpy ΔH of Natural Rubbers

Rubber	ΔH_a,[a] mcal/mg	ΔH_b,[b] mcal/mg
NRSS	101.5	156.6
NRPC	72.7	174.2
Guayule	192.3	167.2

[a] Sample mass 14–15 mg.
[b] Sample mass 3–4 mg.

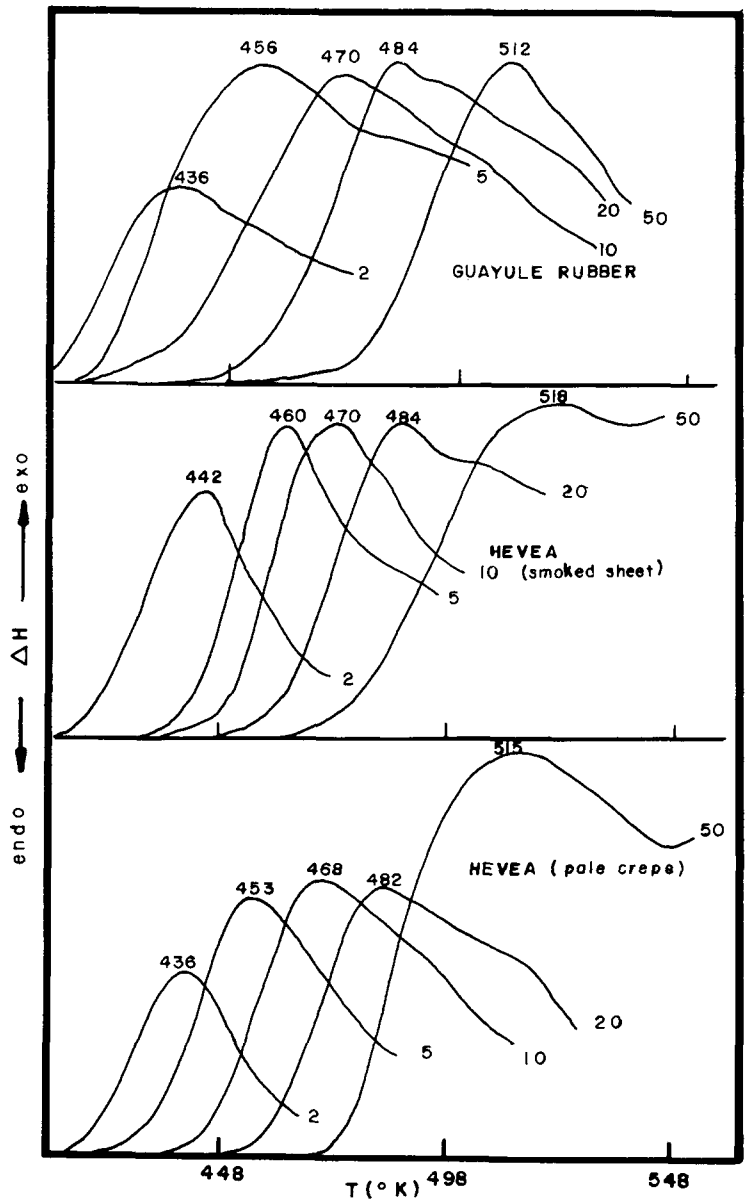

Fig. 4. Influence of heating rate β (°C/min) on the thermogram displacement of the natural rubbers under study.

4, the thermograms studied at several heating rates, ranging between 2 and 50°C/min, are presented. At the highest β value the equilibrium conditions are changed due to the imperfect heat transfer throughout the specimen.

Heat Evolution. In the previous paragraphs, the basic statements of the Borchardt-Daniels model were presented. By using eq. (8) (assuming a first-order reaction) and using the experimental values obtained with the two different masses at a heating rate of 5°C/min, the activation energies were calculated. Table II shows the k values obtained which are presented in graphic form in Figure 5. The good agreement observed for the results obtained with the smaller

TABLE II
Experimental Values for k Obtained Using the Borchardt-Daniels Method[a]

NRSS				NRPC				GR			
M_1 = 15.2 mg		M_2 = 3.4 mg		M_1 = 15.0 mg		M_2 = 3.4 mg		M_1 = 14.8 mg		M_2 = 3.4 mg	
T, °K	k_j	T, °K	k_j	T, °K	k_j	T, °K	k_j	T, °K	k_j	T, °K	k_j
448	3.50×10^{-6}	429	6.00×10^{-7}	437	2.4×10^{-6}	425	6.30×10^{-6}	434	2.2×10^{-6}	425	5.40×10^{-6}
453	4.27×10^{-5}	433	2.21×10^{-6}	442	1.78×10^{-5}	429	5.62×10^{-5}	439	1.57×10^{-5}	429	4.84×10^{-5}
458	1.46×10^{-4}	437	1.20×10^{-4}	447	5.68×10^{-5}	433	2.30×10^{-4}	444	4.07×10^{-5}	433	1.83×10^{-4}
463	3.35×10^{-4}	441	3.61×10^{-4}	452	1.49×10^{-4}	437	5.26×10^{-4}	449	7.73×10^{-5}	437	3.27×10^{-4}
468	5.22×10^{-4}	445	7.27×10^{-4}	457	3.12×10^{-4}	441	9.16×10^{-4}	454	1.17×10^{-4}	441	6.16×10^{-4}
473	7.92×10^{-4}	449	1.25×10^{-3}	462	4.93×10^{-4}	445	1.42×10^{-3}	459	1.70×10^{-4}	445	1.00×10^{-3}
478	1.12×10^{-3}	453	1.83×10^{-3}	467	6.91×10^{-4}	449	1.93×10^{-3}	464	2.23×10^{-4}	449	1.49×10^{-3}
483	1.57×10^{-3}	457	2.47×10^{-3}	472	4.74×10^{-4}	453	2.55×10^{-3}	469	2.91×10^{-4}	453	2.09×10^{-3}
488	2.69×10^{-2}	461	3.13×10^{-3}	477	1.24×10^{-3}	457	2.25×10^{-3}	474	3.44×10^{-4}	457	2.71×10^{-3}
493	2.29×10^{-2}	465	3.90×10^{-3}	482	1.62×10^{-3}	461	3.25×10^{-3}	479	3.19×10^{-4}	461	3.34×10^{-3}
		469	4.94×10^{-3}	487	2.49×10^{-3}	465	4.00×10^{-3}	484	5.24×10^{-4}	465	4.15×10^{-3}
		473	5.89×10^{-3}	492	3.16×10^{-3}	469	4.91×10^{-3}	489	5.79×10^{-4}	469	5.01×10^{-3}
		477	7.38×10^{-3}			473	6.08×10^{-3}	494	7.22×10^{-4}	473	6.13×10^{-3}
		481	9.03×10^{-3}			477	7.41×10^{-3}	499	8.03×10^{-4}	477	7.53×10^{-3}
		485	1.25×10^{-2}			481	8.57×10^{-3}	504	9.31×10^{-4}	481	9.89×10^{-3}
		489	1.41×10^{-2}			485	1.26×10^{-2}	509	1.19×10^{-3}	485	1.29×10^{-2}
						489	2.58×10^{-2}	514	1.22×10^{-3}	489	1.27×10^{-2}
								519	1.35×10^{-3}		

[a] Values were calculated for two different masses at a heating rate of 5°C/min.

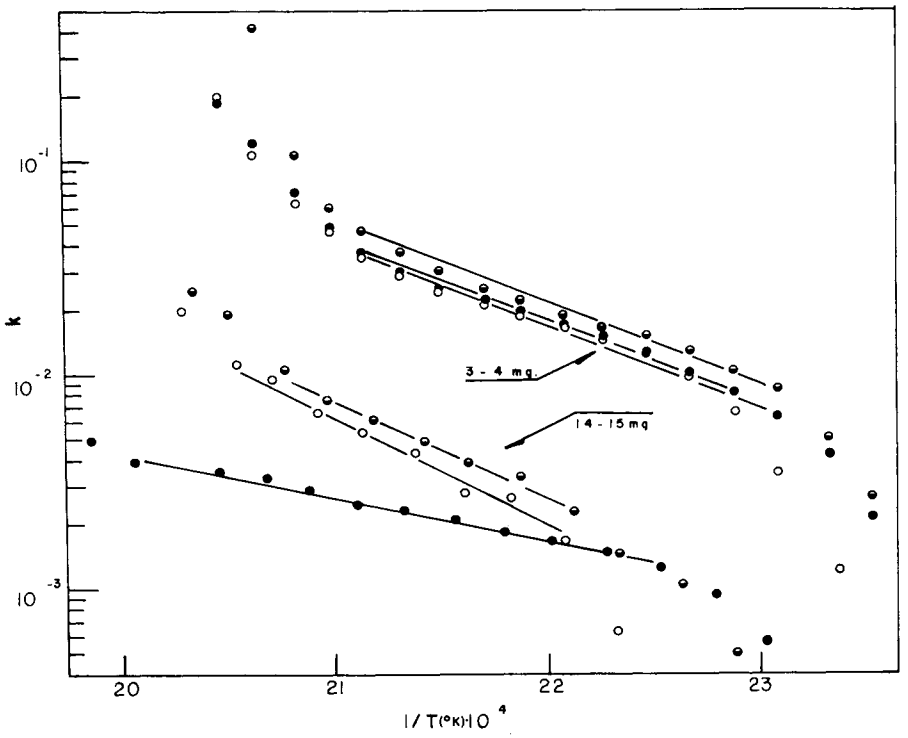

Fig. 5. Graphic presentation showing k values obtained by using the Borchardt-Daniels model plotted vs $1/T$. From the slope the activation energies were calculated by means of the Arrhenius equation: (●) Guayule; (○) smoked sheet; (◒) pale crepe.

mass are different from those obtained with 14–15 mg where the behavior is completely scattered. This will affect the activation energies, the values of which are given in Table V. Linearity is obtained between 433° and 477°K working with samples weighing 3–4 mg and covering the temperature range at which an exothermic oxidation reaction is observed. E_a values obtained by this approach were between 14 and 27 kcal/mole with a 14–15 mg mass and between 16.18 and 16.7 kcal/mole with a 3–4 mg mass.

Controlling Diffusion. Equation (13) was used to mathematically analyze this phenomenon with diffusion arguments. Numerical results are presented in Table III and graphically shown in Figure 6. Good linearity between k and $1/T$ was obtained between 447° and 485°K, a higher temperature interval than that observed in the previous method. The activation energies for the three rubbers were in the order of 21.70–23.42 kcal/mole with 3–4 mg samples, however, with samples in the order of 14–15 mg the range was 17.17–27.9 kcal/mole, a consequence of the inaccuracy introduced when larger masses are used.

Heating Rate. For the determination of the activation energies by the Kissinger and Ozawa method, a β range was explored from 2° to 50°C/min and the results in terms of T_m are presented in Table IV and plotted in Figure 7, from whose slope the activation energies were calculated using eq. (14). This model is independent of the reaction order, and in addition the mass does not present a considerable influence on the E_a values obtained. Activation energies for the two different masses were very close, ranging between 18.0 and 20.6 kcal/mole. Linearity was achieved in all the β values except at 50°C/min. This was probably due to imperfect heat transfer throughout the sample.

TABLE III
Experimental Values for k Using the Jander Equation[a]

NRSS				NRPC				GR			
M_1 = 15.2 mg		M_2 = 3.4 mg		M_1 = 15.0 mg		M_2 = 3.4 mg		M_1 = 14.8 mg		M_2 = 3.4 mg	
T, °K	k_b	T, °K	k_b	T, °K	k_b	T, °K	k_b	T, °K	k_b	T, °K	k_b
488	6.30×10^{-4}	429	1.20×10^{-3}	437	4.90×10^{-4}	425	2.69×10^{-3}	434	5.50×10^{-4}	425	2.03×10^{-3}
453	1.65×10^{-3}	432	3.36×10^{-3}	442	1.04×10^{-3}	429	4.91×10^{-3}	439	9.24×10^{-4}	429	4.30×10^{-3}
458	2.63×10^{-3}	437	6.39×10^{-3}	447	1.54×10^{-3}	433	8.24×10^{-3}	444	1.21×10^{-3}	433	6.57×10^{-3}
463	2.61×10^{-3}	441	9.54×10^{-3}	452	2.34×10^{-3}	437	1.06×10^{-2}	449	1.45×10^{-3}	437	8.12×10^{-3}
468	4.27×10^{-3}	445	1.20×10^{-2}	457	3.29×10^{-3}	441	1.26×10^{-2}	454	1.63×10^{-3}	441	1.00×10^{-2}
473	5.29×10^{-3}	449	1.45×10^{-2}	462	3.95×10^{-3}	445	1.48×10^{-2}	459	1.85×10^{-3}	445	1.22×10^{-2}
478	6.85×10^{-3}	453	1.68×10^{-2}	467	4.69×10^{-3}	449	1.66×10^{-2}	460	2.03×10^{-3}	449	1.45×10^{-2}
483	9.47×10^{-3}	457	1.90×10^{-2}	472	6.02×10^{-3}	453	1.89×10^{-2}	469	2.29×10^{-3}	453	1.70×10^{-2}
488	1.89×10^{-2}	461	2.15×10^{-2}	477	7.41×10^{-3}	457	2.16×10^{-2}	474	2.47×10^{-3}	457	1.94×10^{-2}
493	1.99×10^{-2}	465	2.47×10^{-2}	482	1.02×10^{-2}	461	2.49×10^{-2}	479	2.77×10^{-3}	461	2.19×10^{-2}
		469	2.99×10^{-2}	487	1.09×10^{-2}	465	2.96×10^{-2}	484	3.27×10^{-3}	465	2.59×10^{-2}
		473	3.54×10^{-2}	492	2.48×10^{-2}	469	3.67×10^{-2}	489	3.51×10^{-3}	469	3.01×10^{-2}
		477	4.85×10^{-2}			473	4.64×10^{-2}	494	4.34×10^{-3}	473	3.71×10^{-2}
		481	6.12×10^{-2}			477	5.80×10^{-2}	499	4.89×10^{-3}	477	4.79×10^{-2}
		485	1.05×10^{-1}			481	1.07×10^{-1}	504	4.93×10^{-3}	481	7.10×10^{-2}
		489	1.89×10^{-1}			485	4.01×10^{-1}	509	8.46×10^{-3}	485	1.18×10^{-1}
								514	9.72×10^{-3}	489	1.89×10^{-1}
								519	1.49×10^{-2}		

[a] Values were calculated for two different masses at a heating rate of 5°C/min.

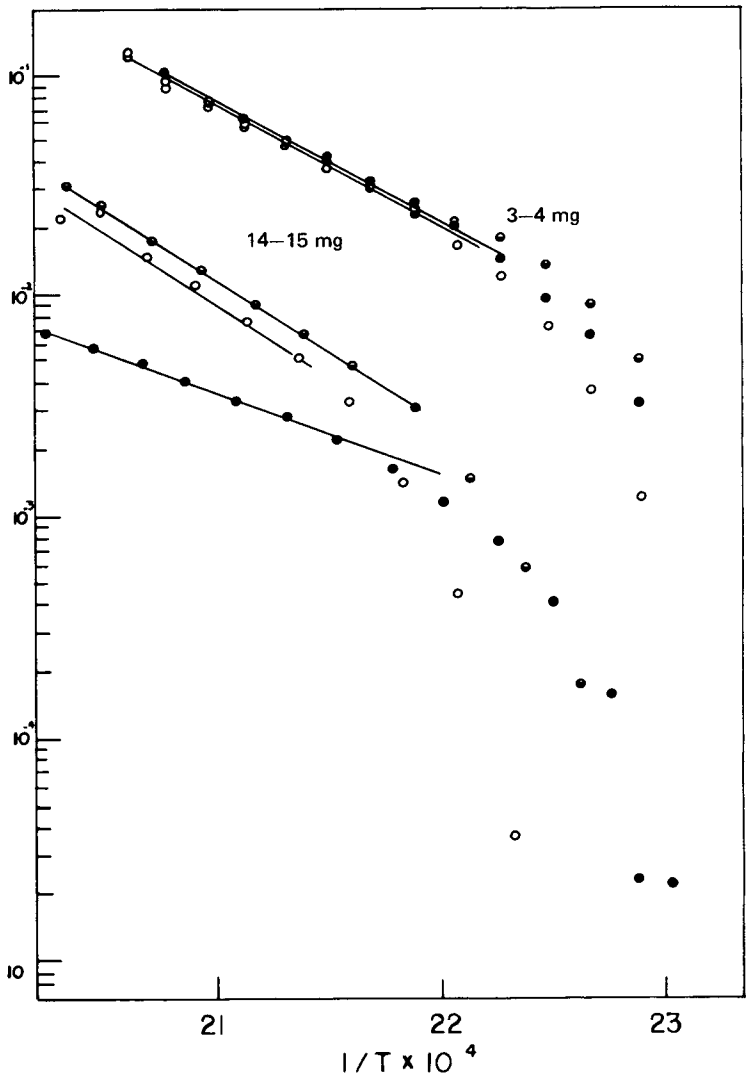

Fig. 6. Graphic presentation showing k values obtained by using the Jander equation (three-dimensional diffusion) plotted vs $1/T$. From the slope the activation energies were estimated by the Arrhenius equation: (○) smoked sheet; (◒) pale crepe; (●) Guayule.

CONCLUSIONS

Results presented and discussed in the previous section showed that in spite of its complexity, the thermal oxidation reactions of Hevea and Guayule natural rubbers can be followed by dynamic differential scanning calorimetry (DSC) and its kinetic characteristics can be determined if the appropriate experimental conditions are used.

An important aspect to be considered with the quantitative analysis of such reactions is the selection of the mathematical tools that are going to be used. The three models applied for the derivation of the kinetic parameters in this work showed good reproducibility using samples ranging between 3 and 4 mg. Borchardt-Daniels, Kissinger-Ozawa, and Jander results are based on different conceptual frameworks, however, the experimental values of the activation

TABLE IV
Experimental Values of T_m obtained at different heating rates

	NRSS		NRPC		GR	
β, °C/min	T_{ma},[a] °K	T_{mb},[b] °K	T_{ma}, °K	T_{mb}, °K	T_{ma}, °K	T_{mb}, °K
2	442.5	429.	436	430	435.5	427
5	460	449	455.5	447	453.0	445
10	470	462	470.0	463	468	459
20	484	478	484	480	482	474
50	518	—	512.0	—	515	—

[a] Temperature value obtained with samples weighing 14–15 mg.
[b] Temperature value obtained with samples weighing 3–4 mg.

energies for each method are in good agreement taking in consideration the difficulties necessary to give appropriate values.[15] Table V summarizes the values obtained; the Borchardt-Daniels model, assuming a first-order reaction, gave an E_a *value* of 17 kcal/mole; Kissinger-Ozawa values were 19 kcal/mole; and Jander values, assuming three-dimensional diffusion, were 22–23 kcal/mole. These values are in good agreement with the 20 kcal/mole obtained by infrared spectroscopy.[6]

From the practical point of view, the Kissinger-Ozawa method presents several advantages over the other models: the mass influence is remarkably lower when compared with Borchardt-Daniels and Jander; an elaborated analysis of the thermogram is not required, and the presence of consecutive reactions does not affect the behavior, however, the kinetic information is reduced in terms so that

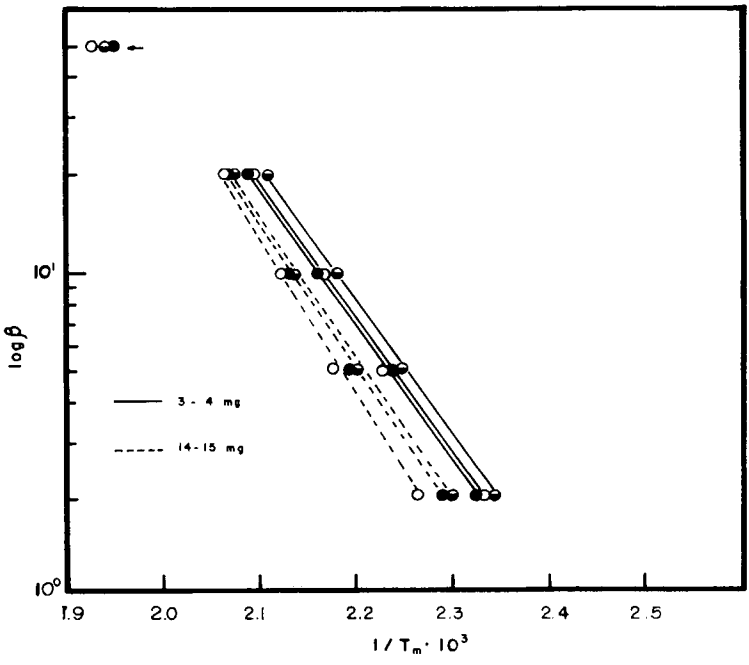

Fig. 7. Plot of log β (°C/min) vs $1/T_m$. From the slope of the lines and using the Kissinger-Ozawa method, the activation energies were calculated: (●) Guayule; (○) Hevea (smoked sheet); (⊖) Hevea (pale crepe).

TABLE V
Activation Energies E_a Obtained for the Three Methods Used and for two Different Masses

	Borchardt-Daniels		Jander		Kissinger-Ozawa	
Rubber	E_a,[a] kcal/mole	E_a,[b] kcal/mole	E_a,[a] kcal/mole	E_a,[b] kcal/mole	E_a,[a] kcal/mole	E_a,[b] kcal/mole
NRSS	27.68	16.18	27.13	21.70	20.60	18.58
NRPC	25.85	16.46	27.98	23.02	19.73	18.82
Guayule	14.06	16.76	17.72	23.42	19.45	18.00

[a] Mass 14–15 mg.
[b] Mass 3–4 mg.

the reaction order cannot be considered and the constant velocity cannot be determined.

Finally, from the thermal oxidation aspect Hevea and Guayule rubber showed identical behavior using DSC and the kinetic values obtained were of the same order of magnitude.

This work was financially supported by the Consejo Nacional de Ciencia y Tecnología (CONACYT) and the Comisión Nacional de las Zonas Aridas (CONAZA). One of the authors (E.C.L.) wishes to thank to the Facultad de Quimica of the Universidad Nacional Autonoma de Mexico for permitting him to stay at CIQA during 1976.

References

1. J. Chiu, *J. Macromol. Sci. Chem.*, **A8**(1), 3 (1974).
2. L. Reich, *J. Appl. Polym. Sci.*, **10**, 1801 (1966).
3. D. A. Smith, *J. Polym. Sci. Polym. Lett.*, **4**, 215 (1966).
4. T. Ozawa, *Bull. Chem. Soc. Jpn.*, **38**, 1881 (1965).
5. K. V. Van, S. L. Malhotra, and L. P. Blanchard, *J. Appl. Polym. Sci.*, **18**, 2671 (1974).
6. J. E. Field, D. E. Woodford, and S. D. Gehman, *J. Polym. Sci.*, **15**, 79, 51 (1955).
7. J. Kello, A. Tkac, and J. Hrevekova, *Rubb. Chem. Technol.*, **29**, 2145 (1956).
8. S. Baxter, W. Mc. G. Morgan, and D. S. P. Roebuck, *Ind. Eng. Chem.*, **43**, 446 (1951).
9. L. J. Kitchen, H. E. Albert, and G. P. Smith, Jr., *Ind. Eng. Chem.*, **42**, 675 (1950).
10. R. B. Spacht, W. S. Hollingshead, and J. G. Lichty, *Rubber World*, **259**, 863 (1959).
11. R. C. Smith and H. L. Stephens, Paper presented at the 105th Meeting of the Rubber Division, Am. Chem. Soc., Toronto, 1974.
12. J. J. Morand, *Rubb. Chem. Technol.*, **47**, 5 (1974).
13. D. C. Blackley, *High Polymer Latices*, Vol. 1, Maclaren, London, 1966, p. 238.
14. E. Campos-López and J. Palacios, *J. Polym. Sci. Polym. Chem.*, **14**, 1561 (1976).
15. A. A. Duswalt, *Thermochim. Acta*, **8**, 57 (1974).
16. L. Reich and S. Stivala, *Elements of Polymer Degradation*, McGraw-Hill, New York, 1971, pp. 81–130.
17. H. E. Kissinger, *J. Res. Natl. Bur. Stand.*, **57**, 217 (1956).
18. H. J. Borchardt and F. Daniels, *J. Am. Chem. Soc.*, **79**, 41 (1957).
19. M. Uricheck, *Perkin-Elmer Instrum. News*, **2**, 17 (1966).
20. T. Ozawa, *J. Therm. Anal.*, to appear.
21. R. C. Mackenzie, *Differential Thermal Analysis*, Vol. 2, Academic Press, New York, 1972, pp. 61–63.
22. F. Skvara and V. Satava, *J. Therm. Anal.*, **2**, 325 (1970).
23. G. Jander and C. Bloom, *Z. Anorg. Chem.*, **258**, 205 (1949).

Received April 25, 1975
Revised January 10, 1977